System Model for a Novel No Moving Parts Diffuser Valve Based Diaphragm Actuated Micro Pump

D. Banerjee*, K. Yano**, S.F. Bart***

*COVENTOR, SAN MATEO, CA 94404, USA. debban@memcad.com
**COVENTOR, Cambridge, MA 02142, USA. kyano@memcad.com
***COVENTOR, Cambridge, MA 02142, USA. sbart@memcad.com

ABSTRACT

Analytical results for oscillating flow in a channel indicate regions of high shear stress close to the wall along with the flow reversal in the central portion of the flow at certain frequencies of actuation. To obviate the huge computational labor and complexity required for an accurate CFD model of an entire micropump, this work describes the formulation of a system model constructed from an extraction of CFD simulation results for compressible and incompressible flows in a no-moving parts diffuser valve for actuation frequencies ranging from 100Hz to 1MHz. The system model was used to predict the optimum frequency of operation from the calculations for flow rate as a function of frequency of actuation of the diaphragm.

Keywords: CFD, system-model, macro-model, micropump, compressible flow.

1. INTRODUCTION

Micro-pumps have been a subject of research since 1980 [1]. Fabrication methods for micropumps have ranged from micro-machining to injection molding to die-casting and materials used have ranged from silicon to brass to plastics. Based on the actuating principles micropumps can be classified as mechanical (jet flow, peristaltic, rotary, centrifugal, reciprocating) and non-mechanical (ultra sound, electrodynamic, electro-osmotic, electrophoretic, electromagnetic, electrostatic, bimetallic). Peristaltic micropumps require active valve mechanisms and use either piezoelectric disk or thermo-pneumatic actuators. Reciprocating micro-pumps, the subject of the present study, have been made in both valve and valve-less configuration and usually use a reciprocating membrane or diaphragm for generating pressure oscillations for driving the fluid. The valve-less pumps rely on the diodicity of flow resistance in certain flow configurations to obtain a temporal average net flow in a particular direction.

The designs of micropumps are challenging in terms of model complexity and limited knowledge of device physics on the microscale. Modeling strategies for micropumps have typically involved CFD simulation [1] and system analyses [1]. Esoteric techniques for modeling of micro-pumps like Monte Carlo simulation [2] and genetic algorithm [3], have also been reported in the literature.

2. ANALYTICAL RESULTS

For understanding fluid flow in a reciprocating diaphragm pump it is essential to analyze flow in a channel for oscillating pressure boundary condition. Figure 1 shows the flow configuration inside an infinite channel with oscillating pressure boundary condition. The governing momentum equation is:

$$\frac{\partial u}{\partial t} = -\frac{1}{\rho}\frac{\partial p}{\partial x} + \nu\frac{\partial^2 u}{\partial y^2} \tag{1}$$

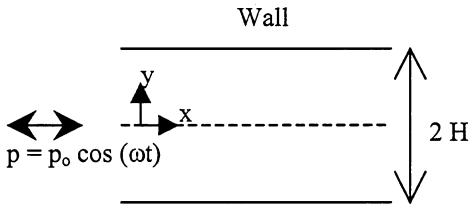

Figure 1. Flow geometry for analytical study of oscillating flow in a semi-infinite channel.

With the pressure transient boundary condition:

$$-\frac{1}{\rho}\frac{\partial p}{\partial x} = Ke^{-i\omega t} \tag{2}$$

and the wall boundary condition at $y=\pm H$ we obtain:

$$u = -i\frac{Ke^{-i\omega t}}{\omega}\left[1 - \frac{\cosh\left(y\sqrt{i\omega/\nu}\right)}{\cosh\left(H\sqrt{i\omega/\nu}\right)}\right] \tag{3}$$

Solving for the flow rate,Φ:

$$\Phi = \int_o^H u\,dy = -i\frac{KHe^{-i\omega t}}{\omega}\left[1 - \sqrt{-i}\frac{l_o}{H}\tanh\left(\frac{H}{l_o}\sqrt{i}\right)\right] \tag{4}$$

The 3dB cutoff frequency, ω_{3dB}, can be obtained by solving for the condition:

$$\Phi / \Phi_{max} = 1/\sqrt{2} \tag{5}$$

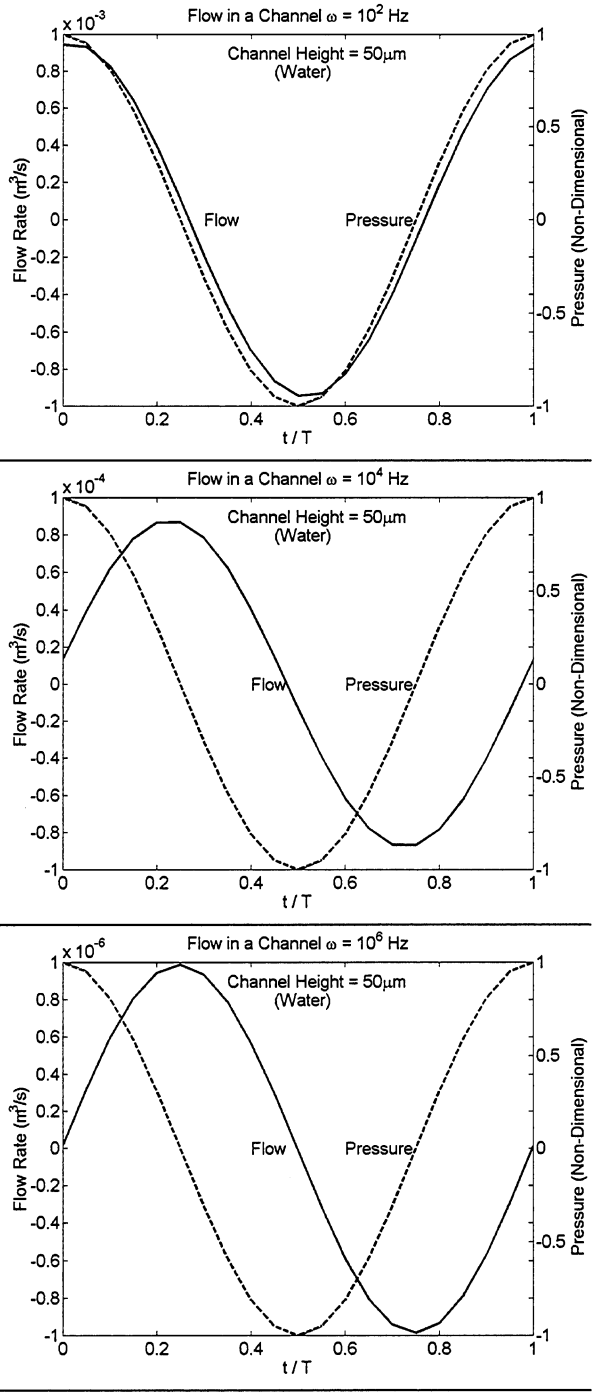

Figure 2: Pressure and flow rate over a cycle at pressure actuation frequency of 100 Hz, 10kHz and 1MHz .

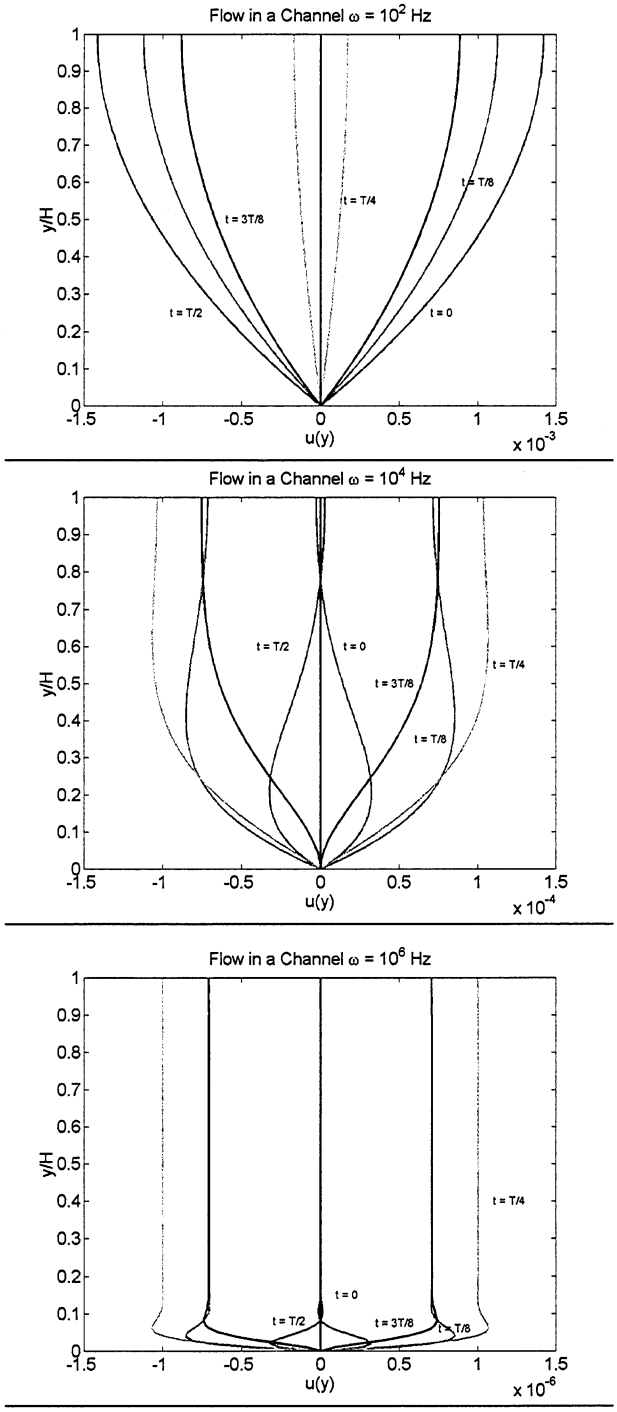

Figure 3: Velocity profiles over a cycle at pressure actuation frequencies of 100Hz, 10KHz and 1MHz.

Here $l_o = \sqrt{\nu/\omega}$ is the characteristic length, K is a constant, ω is the angular frequency of the imposed pressure oscillation, p; H is the half width of the semi-infinite channel, ρ is the density of the fluid, ν is the fluid viscosity, u is the flow velocity and y is the coordinate position in the transverse direction from the centerline of the channel while x is the coordinate location in the flow direction and i is the square root of -1. The values for flow and pressure were obtained from Equations 2, 3 and 4 using Matlab® and plotted in Figures 2, 3 and 4

Figure 2 shows that there is a considerable phase shift in the flow due to viscous damping effects at high frequencies. The flow rate at 1 MHz is 180° out of phase with the actuating pressure signal. Figure 3 shows that the flow profile changes as the actuating frequency is increased. At 100Hz the classic parabolic profile is obtained. However at 10kHz flow reversal is observed at the center of the channel. At 1MHz it is observed that plug flow is obtained a short distance away from the wall. The "boundary layer" is found to shrink as the frequency is increased to 1MHz and flow reversal occurs in this region indicating a high shear stress region near the wall.

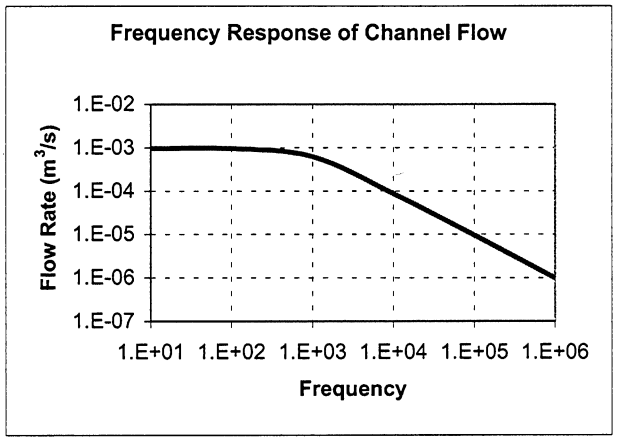

Figure 4: Frequency response for properties of water at normal temperature and pressure for H=50μm.

Also, the plots of flow rate show that the as the actuating frequency is increased by 5 orders of magnitude the flow rate decreases by 3 orders of magnitude. Figure 4 shows the frequency response of channel flow for flow properties of water for H=50mm. Hence a channel acts like a low pass filter – effectively reducing the flow rates at higher frequencies. Equation 5 yields an implicit equation for ω_{3dB} as follows (where, Φ_{max} is for l_o=1):

$$\frac{e^{-i\nu}}{\nu}\left[1-\sqrt{-i}\,\frac{1}{H}\tanh\left(H\sqrt{i}\right)\right] = \frac{e^{-i\omega t}}{\omega}\left[1-\sqrt{-i}\,\frac{l_o}{H}\tanh\left(\frac{H}{l_o}\sqrt{i}\right)\right] \quad (6)$$

For Figure 4, ω_{3dB} = 658 Hz.

The above results show that to effectively use an CFD model large number of grids would be required to accurately resolve the flow reversals and velocity gradients near the wall. Consequently, a CFD model for the whole micropump would involve huge computational labor and long simulation times making it impractical.

3. CFD SIMULATIONS

Figure 5 shows the configuration of the micropump explored in this study. The wedge shaped valves provide directional resistance to flow in the micropump. The bottom surface of the pump consists of an oscillating diaphragm. The net flow occurs from left to right since there is a higher resistance due to flow reversals following the converging direction (nozzle) compared to diverging direction (diffuser) for low wedge angles.

The analyses involved numerical simulations of the valves using Flumecad™ which were used to extract a macromodel for the valves. The macro model extraction was implemented in a system model which was simulated using Matlab®. Numerical simulations were performed on Flumecad™ for 3-D and 2-D incompressible flow for the geometry specified.

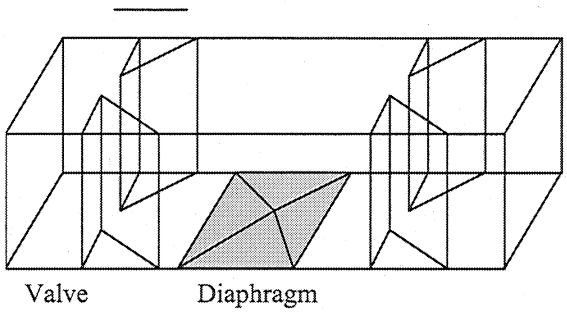

Figure 5: Configuration of micro-pump.

Figure 6 shows a sample result for velocity profile from CFD simulations of 3-D incompressible flow in the micropump. This simulation was performed for the complete pump geometry incorporating the diaphragm, the valves and the pump chamber. The figure shows the velocity vectors during upward movement of the diaphragm such that there is a flow out of the chamber.

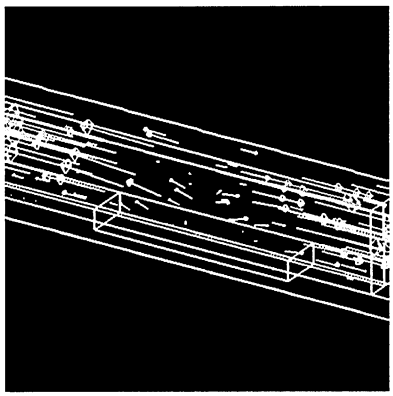

Figure 6: Velocity profiles obtained from CFD simulations for 3-D incompressible flow in the diaphragm pump.

4. SYSTEM MODEL SIMULATIONS

The governing equations describing the system model were obtained from [4] as:

$$\frac{\partial V_{eq}}{\partial p}\bullet\frac{dp}{dt} = \begin{pmatrix}1 & 1\end{pmatrix}\begin{pmatrix}\Phi_l\\ \Phi_r\end{pmatrix} - \frac{\partial V_{dia}}{\partial t} \quad (7)$$

$$\rho_{liquid}\bullet\begin{pmatrix}\alpha_d+\alpha_c & 0\\ 0 & \alpha_d+\alpha_c\end{pmatrix}\bullet\frac{d}{dt}\begin{pmatrix}\Phi_l\\ \Phi_r\end{pmatrix} = \begin{pmatrix}1 & -1 & 0\\ 0 & 1 & 1\end{pmatrix}\bullet\begin{pmatrix}p_{in}\\ p\\ p_{out}\end{pmatrix} - \begin{pmatrix}\Delta p_{loss}(\Phi_l)\\ \Delta p_{loss}(\Phi_r)\end{pmatrix} \quad (8)$$

$$\frac{\partial V_{eq}}{\partial p} = \kappa_{liquid}V_{ch} + \left(\frac{1}{p+p_o}-\kappa_{liquid}\right)\bullet\frac{xV_{ch}p_0}{p+p_0} \quad (9)$$

Here: p is the pressure, and Δp_{loss} is the pressure loss in the tubes, t is time, V_{ch} is the chamber volume at rest, V_{dia} is the diaphragm swept volume, V_{eq} is the effective volume of the chamber, x is the mass fraction of vapor in the chamber due to cavitation (taken to be zero in the present model), α is the volume flow rate correction factor (arising from non-uniform distribution of velocity across the nozzle cross-section, Φ is the volume flow rate, and κ is the liquid compressibility. Also, subscripts c and d referring to diodicity in nozzle and diffuser mode of operations, l and r refer to the left and right side nozzles, respectively.

The notable aspect of this model is that a pressure drop regulator was designed to minimize growth of the numerical instabilities in the solution of the simultaneous differential equations and is shown in Figure 7. The regulator was used to reset the pressure drop to the maximum value possible in case of overshoot in the calculations for pressure drop values.

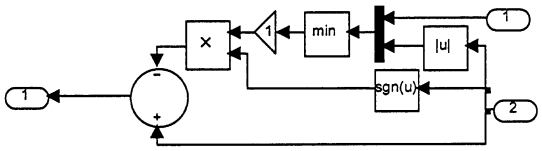

Figure 7: Numerical implementation of a pressure regulator in the system model for the micropump.

System modeling tools provide a convenient approach to integrating various domains of a design process where the interaction between various sub-systems can be analyzed with desired degrees of intricacy in a top-down approach. From such a model the frequency response of the net time averaged flow rate of the micro-pump can be determined.

The system model enabled a much faster method (compared to CFD simulations) for obtaining the flow rate as a function of operating frequency of the pump, as shown below. For the dimensions and operational characteristics specified for the micro-pump, the chamber volume is 3.2nl and the diaphragm swept volume is 0.4 nl. Two models were incorporated in the analyses: incompressible flow and compressible flow. The figure shows that the flow rates predicted by the incompressible flow and the compressible flow model are different for lower frequencies. This is because of the nature of the governing equations employed in the two models, which make them divergent for lower frequencies of operation as well. The incompressible flow model yields a flow rate of 0.011nl/s, which is independent of frequency. The compressible model yields the frequency response of the micro-pump. The figure shows that the pump has an optimum operational frequency range from 200 Hz to 5kHz. Below 200 Hz and above 5 kHz there is a sharp drop in the flow rate. The maximum flow rate obtainable by this design is 0.023 nl/s at a frequency of 800 Hz.

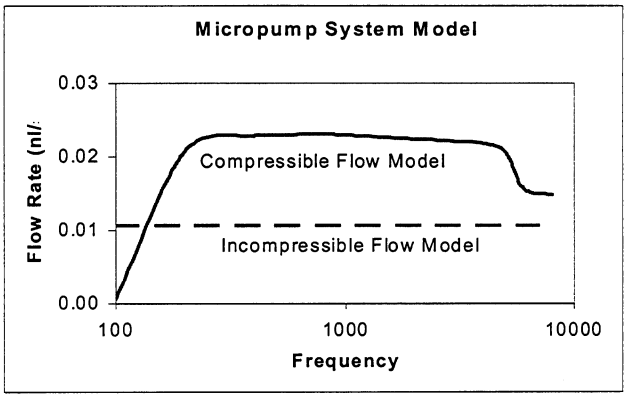

Figure 8 System model for results for compressible and incompressible flow in a micropump.

5. CONCLUSIONS

1. Analytical results showed that for oscillating flow in a channel, the flow regimes are characterized by high shear stress regions near the wall and flow reversal regions near the center for high actuation frequencies. The flow rate is also found to be out of phase with the imposed pressure oscillation due to viscous damping.
2. Velocity and pressure distribution at various actuation frequencies were obtained using CFD simulations.
3. A system model was used to calculate the flow rate of the pump as a function of the actuation frequency.
4. Results from the system model show that the optimal frequency range of operation of the micropump is from 200 Hz to 5kHz for compressible flow regimes. For incompressible flow the flow rate was found to be independent of frequency, as would be expected. The optimal frequency of operation was found to be 800Hz and the maximum flow rate attainable by the micropump was found to be 0.023nl/s for a chamber volume of 3.2nl and piston displacement of 0.8nl.

ACKOLEDGEMENT

The authors would like to thank R. Yamamoto and N. Matsumoto, Fuji Photo Film Co., for useful discussions.

REFERENCES

[1] Gravensen et. al., "Microfluidics – a review", *Journal of Micromechanics and Microengineering*, Vol. 3, pp. 168-182, 1993.

[2] Piekos, E., and Breuer K.S., "DSMC Modelling of Micromechanical devices", *AIAA Paper No. 95-2089*, 1995.

[3] Sharatchandra, M.C., Sen, M., Gad-el-Hak, M., "A New Approach to Constrained Shape Optimization Using Genetic Algorithms", *AIAA Journal*, Vol. 36, No. 1, Jan. 1998.

[4] Olsson, A., "Valve-less Diffuser Micropumps", Ph.D. thesis, Royal Institute of Technology, Stockholm, 1998.